PLOS ONE

RESEARCH ARTICLE

Bruch's membrane opening minimum rim width and retinal nerve fiber layer thickness in a Brazilian population of healthy subjects

Camila S. Zangalli[1]*, Jayme R. Vianna[2], Alexandre S. C. Reis[1], Jamil Miguel-Neto[1], Claude F. Burgoyne[3], Balwantray C. Chauhan[2], Vital P. Costa[1]

1 Department of Ophthalmology, University of Campinas, Campinas, Brazil, **2** Department of Ophthalmology and Visual Sciences, Dalhousie University, Halifax, NS, Canada, **3** Optic Nerve Head Research Laboratory, Devers Eye Institute, Portland, OR, United States of America

* czangalli@gmail.com

Check for updates

OPEN ACCESS

Citation: Zangalli CS, Vianna JR, Reis ASC, Miguel-Neto J, Burgoyne CF, Chauhan BC, et al. (2018) Bruch's membrane opening minimum rim width and retinal nerve fiber layer thickness in a Brazilian population of healthy subjects. PLoS ONE 13(12): e0206887. https://doi.org/10.1371/journal.pone.0206887

Editor: Sanjoy Bhattacharya, Bascom Palmer Eye Institute, UNITED STATES

Received: February 17, 2018

Accepted: October 23, 2018

Published: December 18, 2018

Copyright: © 2018 Zangalli et al. This is an open access article distributed under the terms of the Creative Commons Attribution License, which permits unrestricted use, distribution, and reproduction in any medium, provided the original author and source are credited.

Data Availability Statement: All relevant data are within the paper and its Supporting Information files.

Funding: Camila Zangalli was funded by the Conselho Nacional de Desenvolvimento Científico e Tecnológico (CNPq); J. Vianna: None; A. Reis: None; J. Neto: None; C. Burgoyne: NIH/NEI R01-EY021281; Legacy Good Samaritan Foundation; Heidelberg Engineering, GmbH, Heidelberg, Germany; B. Chauhan: Heidelberg Engineering,

Abstract

Objective

To determine Bruch's membrane opening (BMO) minimum rim width (MRW) and peripapillary retinal nerve fiber layer thickness (RNFLT) measurements, acquired with optical coherence tomography (OCT) in healthy Brazilian individuals self-reported as African Descent (AD), European Descent (ED) and Mixed Descent (MD).

Methods

260 healthy individuals (78 AD, 103 ED and 79 MD) were included in this cross-sectional study conducted at the Clinics Hospital of the University of Campinas. We obtained optic nerve head (24 radial B scans) and peripapillary retinal nerve fiber layer (3.5-mm circle scan) images in one randomly selected eye of each subject.

Results

After adjustment for BMO area and age, there were no significant differences in mean global MRW (P = 0.63) or RNFLT (P = 0.07) among the three groups. Regionally, there were no significant differences in either MRW or RNFLT in most sectors, except in the superonasal sector, in which both MRW and RNFLT were thinner among ED (P = 0.04, P<0.001, respectively). RNFLT was also thinner in ED in the inferonasal sector (P = 0.009). In all races, global MRW decreased and global RNFLT increased with BMO area. AD subjects had higher rates of global RNFLT decay with age (-0.32 μm/year) compared to ED and MD subjects (-0.10 μm/year and -0.08 μm/year, respectively; P = 0.01 and P = 0.02, respectively).

Conclusions and relevance

While we found no significant differences in global MRW and RNFLT among the three races, age-related thinning of the RNFLT was significantly higher in the AD subgroup, which warrants further study.

GmbH, Heidelberg, Germany; Dalhousie Medical Research Foundation; Allergan; V. Costa: None. Drs. Burgoyne and Chauhan are consultants to Heidelberg Engineering. In this role, they receive unrestricted research support, instruments, software, and occasional travel support. This does not alter our adherence to PLOS ONE policies on sharing data and materials. Both hold no patents and receive no honorariums or personal income. The above listed sponsors/funding organizations had no role in the design or conduct of this research.

Competing interests: C. Zangalli: None; J. Vianna: None; A. Reis: None; J. Neto: None; C. Burgoyne: NIH/NEI R01-EY021281; Legacy Good Samaritan Foundation; Heidelberg Engineering, GmbH, Heidelberg, Germany; B. Chauhan: Heidelberg Engineering, GmbH, Heidelberg, Germany; Dalhousie Medical Research Foundation; Allergan; V. Costa: None. Drs. Burgoyne and Chauhan are consultants to Heidelberg Engineering. In this role, they receive unrestricted research support, instruments, software, and occasional travel support. This does not alter our adherence to PLOS ONE policies on sharing data and materials.

Introduction

Assessment of the optic nerve head (ONH) is vital for the detection and follow-up of glaucoma damage. Conventionally, clinical [1] and instrument-based [2–6] evaluation of the ONH estimate the ONH neuroretinal rim in the plane of the visible optic disc margin. However, using optical coherence tomography (OCT), a series of studies have shown that the disc margin is not a consistent OCT anatomic landmark contributing to errors in rim parameters, and that for OCT rim assessment, Bruch's membrane opening (BMO) is a more suitable landmark [7, 8]. OCT BMO Minimum Rim Width (MRW) is a parameter that uses BMO as the anatomic reference point and MRW is defined as the shortest distance between BMO and the internal limiting membrane, in effect, measuring the neuroretinal rim perpendicular to the trajectory of the overlying rim tissue [9, 10]. It therefore takes into account the orientation of the RGC axons as they pass through BMO to enter the anterior neural canal. MRW measurements have demonstrated better diagnostic performance for detecting glaucoma than other rim parameters [11] and better structure-function relationships [12] with visual field testing.

In addition to this new parameter, acquisition and regionalization of data is now based on the subject's individual fovea to BMO center (FoBMO) axis, which is highly variable among subjects [13, 14]. ONH phenotyping with MRW has recently been described in Caucasians [15, 16] and African Americans [16] from the US and Europe. However, ONH phenotypes may vary considerably in healthy subjects across other racial groups. Marsh and colleagues have shown that individuals of European Descent (ED) have significantly smaller optic disc areas (based on the clinically visible optic disc margin) than Hispanics and African Americans [17]. Similarly, Girkin and colleagues found that African Descents (AD) have larger optic discs areas compared to ED [18]. The same authors also showed that retinal nerve fiber layer thickness (RNFLT) varies by quadrant across racial groups: ED individuals had the thinnest RNFLT measurements except in the temporal quadrant, corresponding to the papillomacular bundle, which was thinner in the AD group [18].

The majority of the Brazilian population is the product of three ancestral roots: Europeans, Africans, and Amerindians and miscegenation among these groups is highly prevalent [19]. Furthermore, ADs from Brazil have emigrated from different regions of Africa compared to those who migrated to the US.[20–22] Therefore, it may well be that the ONH phenotypic characteristics of the Brazilian population may not be comparable to those of other countries and may differ from OCT databases currently being used. The purpose of this study was to determine MRW and RNFLT measurements in a normal Brazilian population of self-reported AD, ED and MD (individuals who reported both European and African ancestry). In addition, we evaluated the effects of age and ONH anatomy on these parameters.

Materials and methods

Participants

This was a prospective, cross-sectional, observational study approved by the Institutional Review Board of the University of Campinas (approval number 946.742) and conducted in accordance with the Declaration of Helsinki. Healthy subjects aged between 18 and 80 years, of both sexes, were recruited at the Clinics Hospital of the University of Campinas, São Paulo. Participants were either hospital employees or patients' family members. We aimed to recruit 15 to 20 subjects in each decade of life.

The inclusion criteria were: (1) age between 18 and 80 years-old, (2) best-corrected visual acuity (BCVA) $\geq$ 20/40, (3) refractive error within ± 6.0 spherical diopters and $\leq$ 2.0 cylinder diopters, (4) intraocular pressure (IOP) $\leq$ 21 mmHg, (5) normal clinical eye examination with

a normal appearing optic disc (both eyes had to have intact neuroretinal rims and no disc hemorrhage, notch, localized pallor, or cup-to-disc ratio asymmetry > 0.2), and (6) normal visual fields (Glaucoma Hemifield Test, mean deviation and pattern standard deviation within normal limits). Exclusion criteria were: (1) clinically significant vitreoretinal, neuro-ophthalmological or choroidal diseases, (2) uveitis, (3) prior refractive surgery or intraocular surgery, except for non-complicated cataract, (4) subjects with a history of ocular hypertension, angle closure or glaucoma suspect diagnosis in either eye, (5) unreliable visual fields (false positive rate $\geq$ 15% and false negative rate $\geq$ 20%) and (6) poor quality OCT images (signal strength < 20). Participants were allowed to repeat the visual field once if the results were unreliable. If both eyes were eligible, one eye was randomly selected as the study eye.

Procedures

After oral and written informed consent was obtained, participants underwent a complete ophthalmic examination, which included a review of medical history, automated refraction (Topcon AR RM-8000B, Topcon, Tokyo, Japan), best-corrected visual acuity, slit-lamp biomicroscopy, IOP measurement with Goldmann applanation tonometry, gonioscopy, undilated funduscopic examination with a handheld 78 diopter lens, axial length and central corneal thickness measurement (Lenstar LS900, Haag-Streit AG, Koeniz, Switzerland), automated perimetry (SITA standard 24–2, Humphrey Field Analyzer, Carl Zeiss Meditec Inc, Dublin, CA) and OCT (Spectralis, version 6.0.10.0, Heidelberg Engineering, Heidelberg, Germany) imaging. Self-reported race also was recorded. Only individuals who reported being AD, ED or MD (who comprised both European and African ancestry) were included in the study. Participants were examined between November, 2014 and October, 2016.

Spectral-domain optical coherence tomography

The ONH and peripapillary RNFL were imaged with a scan speed of 40,000 A-scans/second. The acquisition protocol has been detailed elsewhere [15]. Briefly, 2 scan patterns were obtained: ONH (24 radial scans centered on BMO) and peripapillary scans (3 concentric circle scans of 3.5, 4 and 4.5 mm in diameter). Both scans were acquired relative to its eye-specific FoBMO axis, which was determined before the acquisition. For the 24 radial B-scans, settings were fixed at 15˚, 768 A-scans per B-scan, with each B-scan representing an average of 25 scans. For the circle scans, settings were fixed at 3.5, 4 and 4.5 mm diameters centered on the BMO, 768 A-scans, with each circle scan averaged 100 times (**Fig 1**). Only the 3.5 mm circle scan was used for analysis. All participants were imaged by one experienced examiner (C.S.Z.), who also checked all automatic segmentations and manually corrected the BMO, ILM and RNFL segmentations in the 24 radial scans and in the 3.5mm circle scans, when necessary. We chose to have only one examiner since both RNFLT and MRW have shown excellent intra- and interobserver reproducibility on a previous study published by our group [23]. The following parameters were evaluated and automatically generated by the Heidelberg software (version 1.9.13.0): FoBMO Angle, BMO area, MRW and RNFLT.

Analysis

The following parameters were evaluated: FoBMO Angle, BMO area, MRW and RNFLT. MRW and RNFLT measurements were averaged and analyzed globally and in 6 sectors: four of 40˚ (superonasal, inferonasal, inferotemporal, superotemporal), one of 90˚ (temporal), and one of 110˚ (nasal) [24]. All measurements were regionalized relative to the subjects' FoBMO axis. Demographic and ocular parameters were compared among groups with one-way analysis of variance (ANOVA). Analysis of covariance (ANCOVA) was conducted to evaluate mean

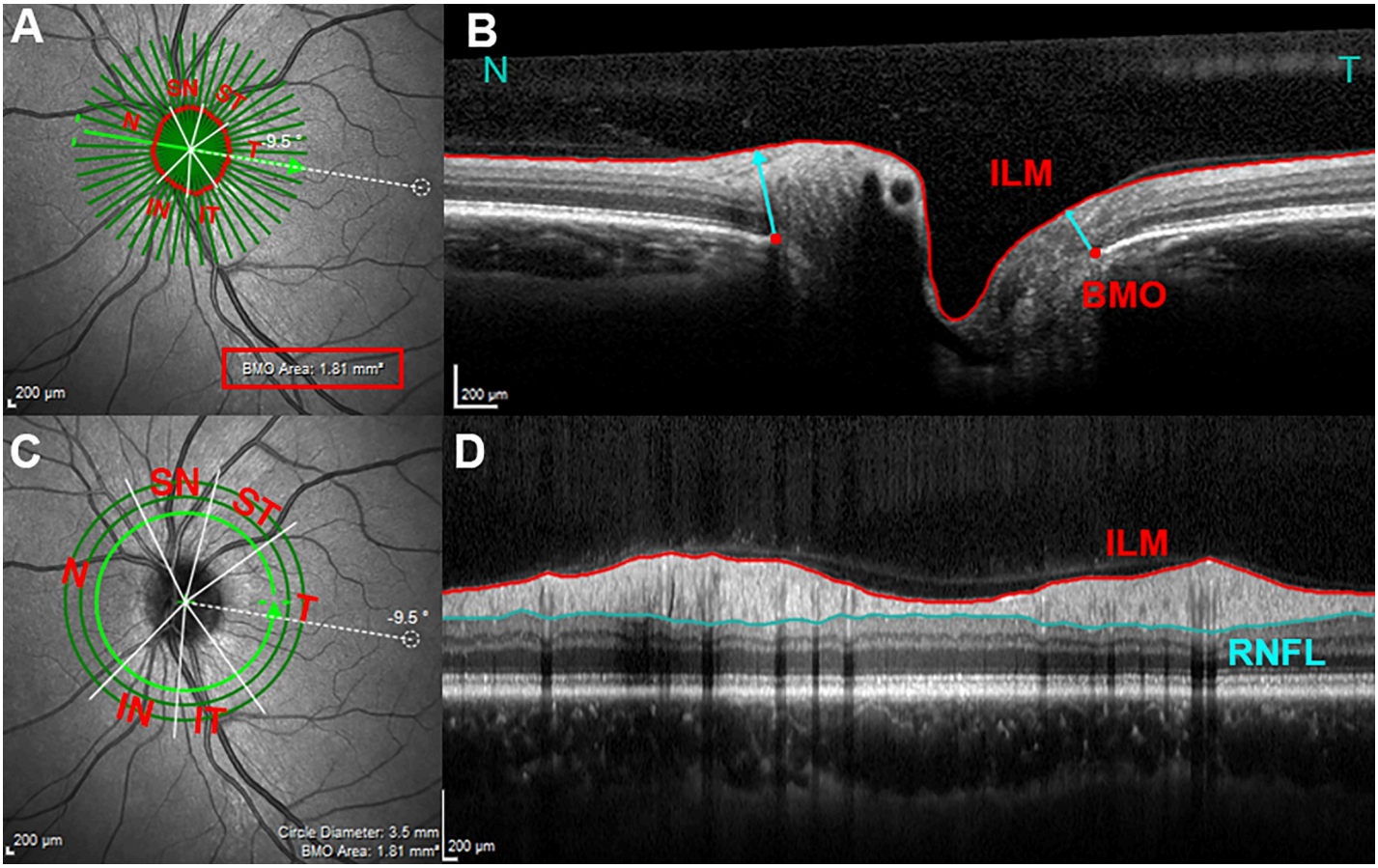

Fig 1. Spectral-domain optical coherence tomography imaging and parameters' measurements. The infrared image in (A) shows 24 radial B-scans centered on the ONH (dark green radial lines) acquired relative to the orientation of the FoBMO center axis (green arrow connecting the fovea and the BMO center, -9.5˚ in this subject). In (B), one horizontal radial B scan shows MRW measurements. MRW (cyan arrow) is the minimum distance between BMO (red dots) and ILM (delineated in red). Each B scan yield 2 BMO points and 2 MRW measurements, in this example a nasal (N) and a temporal (T) measurement. The 3D coordinates of each of the 48 BMO points are used to fit a spline which derives a closed curve representing the BMO area (1.81 mm in this disc). In (C) the 3.5 mm diameter circular scan (light green circle) centered on the ONH was used for RNFLT measurements. (D) Is the corresponding circular B-scan showing the ILM (red) and RNFL (cyan) delineations. MRW and RNFLT measurements were averaged and analyzed globally and in 6 sectors: ST(superotemporal), SN (superonasal), IT (inferotemporal), IN (inferonasal), T (temporal), and N (nasal), in relation to the FoBMO center axis.

https://doi.org/10.1371/journal.pone.0206887.g001

differences in RNFLT and MRW among the three racial groups, adjusting for age and BMO area. The chi-square test was used for categorical variables. We used multivariable linear regression models with interaction terms to evaluate if the effects of co-variables, such as age and BMO area, on MRW or RNFLT. Measurements were adjusted for age and BMO area since previous studies have shown a significant association between both parameters (RNFLT and MRW) and BMO area and age, in normal individuals [15, 16]. We evaluated the relationship between sectorial MRW and RNFLT, adjusted for BMO area, age and race. Partial R^2 values estimating the relative importance of each predictor were reported [25]. The sectorial age-related loss of MRW and RNFLT was calculated and reported as the percentage loss. Data analysis was performed with the open-source software R [26].

Results

Among the 304 individuals recruited, 44 were excluded for the following reasons: abnormal or non-reliable visual fields (n = 18), visually significant cataract (BCVA<20/40) (n = 2), diabetic

Table 1. Clinical characteristics of study subjects.

	All (n = 260)	ED (n = 103)	AD (n = 78)	MD (n = 79)	*P**
Age, years	44.90 (14.5) [17.8–79.3]	46.49 (15.23) [17.8–78.3]	43.92 (15.12) [18.1–79.3]	43.8 (12.78) [19.7–68.6]	0.36
Gender F/M, %	60/40	60/40	63/37	59/41	0.90
CCT, μm	531.26 (33.63) [442–635]	535.75 (32.0) [454–635]	526.58 (35.3) [454–596]	530.14 (33.57) [442–609]	0.17
AXL, mm	23.46 (0.96) [21.02–27.59]	23.47 (0.99) [21.02–27.59]	23.55 (0.88) [22.01–25.56]	23.36 (0.99) [21.15–26.02]	0.45
FoBMO (˚)	-6.54 (3.71) [-15.32–3.72]	-6.96 (3.83) [-15.19–2.66]	-5.96 (3.69) [-15.17–2.30]	-6.56 (3.55) [-15.32–3.72]	0.20
BMO area, mm^2	1.92 (0.43) [0.98–3.69]	1.86 (0.41) [0.98–3.37]	1.98 (0.48) [1.15–3.69]	1.93 (0.40) [0.99–3.31]	0.16

Values shown are mean (standard deviation) and [range].

ED: European descent; AD: African descent; MD: Mixed descent; CCT: central cornea thickness; AXL: axial length; MRW: minimum rim width; BMO: Bruch's membrane opening; RNFLT: retinal nerve fiber layer thickness

*ANOVA was used for all variables, except gender, which was analyzed with Chi-square test.

https://doi.org/10.1371/journal.pone.0206887.t001

retinopathy (n = 2), epirretinal membrane (n = 1), age-related macular degeneration (n = 1), low quality OCT scan (n = 2), chorioretinal macular scar (n = 1), optic disc hypoplasia (n = 1) and glaucoma suspect (n = 14). Therefore, a total of 260 (85.5%) participants were included in the analysis, of whom 78 (30%) were self-identified as AD, 103 (40%) as ED and 79 (30%) as MD. There were between 17 and 21 ED, 14 and 19 AD and 15 and18 MD participants in each decade group, except for the 8th decade, which included 7 subjects in the ED group, 3 in the AD group and no participants in the MD group.

Overall, the mean age was 44.9 years old and 60% were female. There were no significant differences among the racial groups in the measured demographic and ocular characteristics (Table 1). The BMO areas among the three groups were not significantly different (Table 1 and Fig 2). Fig 3 shows the MRW and RNFLT profiles for the three groups. There were no significant differences in mean global MRW among the three racial groups (P = 0.63, Table 2).

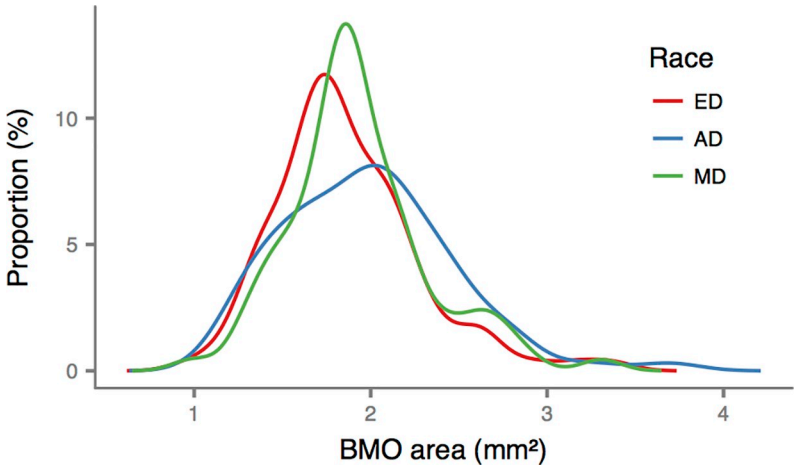

Fig 2. Smoothed histogram showing the distribution of Bruch's membrane opening (BMO) areas for each race. ED: European Descent; AD: African Descent; MD: Mixed Descent.

https://doi.org/10.1371/journal.pone.0206887.g002

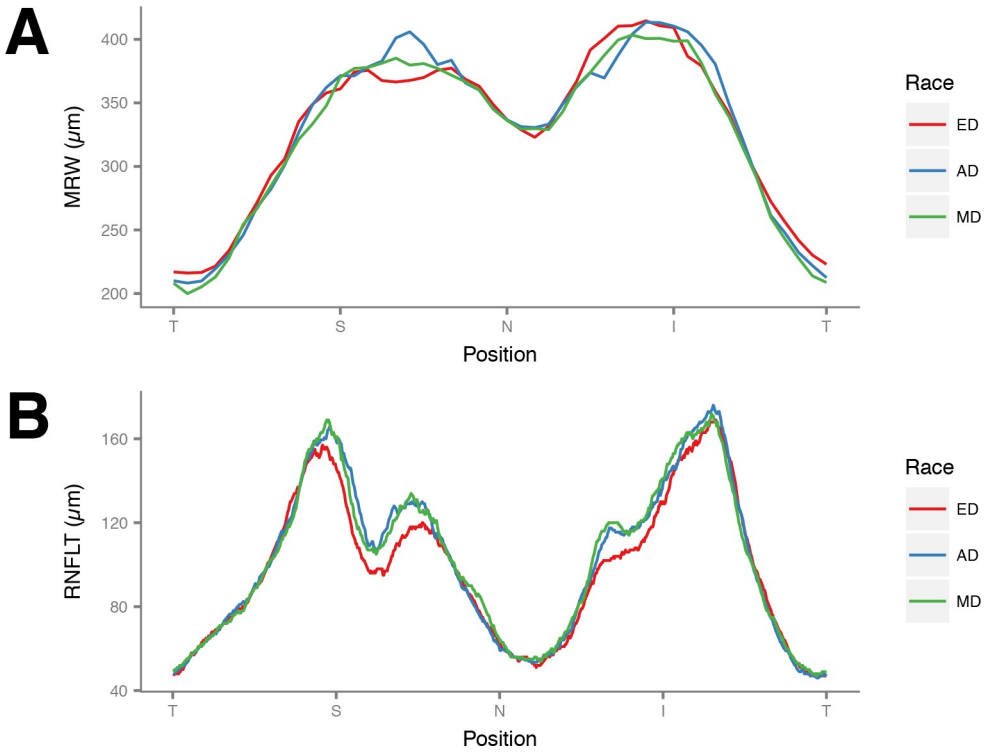

Fig 3. Graphs showing (A) minimum rim width (MRW) and (B) peripapillary retinal nerve fiber layer thickness (RNFLT) profiles for each race. ED: European Descent; AD: African Descent; MD: Mixed Descent. T: temporal; S: superior; N: nasal; I: inferior.

https://doi.org/10.1371/journal.pone.0206887.g003

Mean global RNFLT was thinner in ED (P = 0.01), but this difference was statistically eliminated after adjusting for BMO area and age (P = 0.07, Table 3). In regional analysis, however, after adjusting for BMO area and age, both MRW and RNFLT were greater in AD in the superonasal sector (P = 0.04, P<0.001, respectively) while RNFLT was greater among AD and MD in the inferonasal sector (P = 0.009, **Tables 2 and 3**).

Table 2. Comparison of global and sectorial minimum rim width (MRW) measurements by race.

	ED (n = 103)	AD (n = 78)	MD (n = 79)	*P**	*P* Adjusted**
Global	334.06 (50.15) [242.02–460.84]	335.5 (56.63) [223.69–478.85]	328.12 (50.71) [236.96–487.77]	0.63	0.34
Temporal	236.83 (45.44) [130.8–358.37]	235.3 (54.35) [120.05–361.61]	230.41 (44.89) [134.45–335.04]	0.65	0.51
Superotemporal	319.88 (52.62) [202.04–447.14]	323.75 (60.01) [155.75–469.12]	314.41 (52.76) [198.77–448.65]	0.56	0.36
Inferotemporal	360.17 (60.34) [245.44–574.53]	365.92 (66.58) [221.91–520.98]	352.07 (59.39) [242.98–518.89]	0.37	0.19
Nasal	365.86 (61.46) [247.7–518.23]	364.16 (71.15) [232.31–559.57]	360.09 (67.53) [217.94–585.92]	0.84	0.64
Superonasal	374.05 (66.74) [221.19–574.36]	391.92 (72.37) [264.43–541.16]	375.57 (66.87) [216.52–513.56]	0.17	**0.04**
Inferonasal	413.52 (69.49) [275.88–586.47]	407.09 (74.1) [248.17–604.78]	402.38 (65.00) [285.09–619.11]	0.55	0.45

Values shown are mean (standard deviation) and [range] in μm.

ED: European descent; AD: African descent; MD: Mixed descent

*ANOVA

**ANCOVA to evaluate mean differences in MRW between the three racial groups correcting for age and BMO area.

P values < 0.05 are shown in bold.

https://doi.org/10.1371/journal.pone.0206887.t002

Table 3. Comparison of global and sectorial retinal nerve fiber layer thickness (RNFLT) measurements by race.

	ED (n = 103)	AD (n = 78)	MD (n = 79)	*P**	*P* Adjusted**
Global	99.59 (9.57) [81–129]	103.53 (11.59) [74–132]	103.52 (9.64) [65–130]	**0.01**	0.07
Temporal	68.2 (10.45) [45 – 101]	68.18 (11.91) [32 – 107]	68.66 (9.53) [46 – 95]	0.94	0.73
Superotemporal	128.42 (22.27) [76–172]	128.67 (24.57) [70–195]	128.8 (21.58) [76–175]	0.99	0.82
Inferotemporal	154.24 (19.39) [117–212]	157.14 (20.41) [93–211]	155.7 (18.84) [75–198]	0.61	0.95
Nasal	82.9 (13.13) [55 – 122]	85.21 (15.57) [48 – 127]	86.47 (11.12) [61–116]	0.18	0.38
Superonasal	116.72 (23.83) [66–198]	134.51 (28.07) [83–214]	127.87 (21.6) [74–183]	**<0.001**	**<0.001**
Inferonasal	116.52 (23.11) [65–185]	124.12 (21.55) [78–178]	127.81 (22.52) [72–200]	**0.003**	**0.009**

Values shown are mean (standard deviation) and [range] in μm.

ED: European descent; AD: African descent; MD: Mixed descent

*ANOVA

**ANCOVA to evaluate mean differences in RNFLT between the three racial groups correcting for age and BMO area.

P values<0.05 are shown in bold.

https://doi.org/10.1371/journal.pone.0206887.t003

Global MRW declined significantly with age, after adjusting for BMO area, in AD (-1.45 μm/year; P<0.01 versus 0), the amount by which was not different in ED (-1.28 μm/year; P = 0.71) or MD (-1.34 μm/year; P = 0.83). The rate of global MRW with age was similar in ED and MD (P = 0.91; Table 4). The age-related reduction of global RNFLT, adjusted for BMO area, was significant in AD (-0.32 μm/year; P<0.01 versus 0) and was faster than that compared to ED (-0.10 μm/year, P = 0.01) or MD (-0.08 μm/y, P = 0.02). The rate of global RNFLT reduction with age was similar in ED and MD (P = 0.86; Table 4 and Fig 4).

After adjusting for age, global MRW declined significantly with BMO area in AD (-38.51 μm/mm^2), and this relationship was not different in ED (-60.56 μm/mm^2, P = 0.15) and MD (-57.04 μm/mm^2, P = 0.26). The rates of global MRW reduction were also similar

Table 4. Multivariable regression models evaluating the relationship between minimum rim width (MRW) and peripapillary retinal nerve fiber layer thickness (RNFLT) and covariates by racial group.

	ß (95% CI)			*P* value		
	AD	**ED**	**MD**	**AD vs ED**	**AD vs MD**	**ED vs MD**
MRW						
Age* (μm/y)	-1.45 (-2.12, 0.79)	-1.28 (-1.87, -0.70)	-1.34 (-2.12, -0.56)	0.71	0.83	0.91
BMO area (μm/mm^2)**	-38.51 (-59.28, -17.74)	-60.56 (-82.24, -38.88)	-57.04 (-82.00, -32.08)	0.15	0.26	0.83
RNFLT* (μm/μm)**	2.05 (1.20, 2.90)	1.60 (0.67, 2.54)	1.72 (0.71, 2.74)	0.45	0.61	0.85
RNFLT						
Age* (μm/y)	-0.32 (-0.45, -0.19)	-0.10 (-0.21, 0.02)	-0.08 (-0.23, 0.07)	**0.01**	**0.02**	0.86
BMO area (μm/mm^2)**	8.57 (4.48, 12.67)	11.33 (7.05, 15.60)	11.81 (6.88, 16.73)	0.15	0.26	0.83

AD: African descent; ED: European descent; MD: Mixed descent; BMO: Bruch's membrane opening

*Adjusted for BMO area

**Adjusted for age

*** Adjusted for age and BMO area

P values < 0.05 are shown in bold.

https://doi.org/10.1371/journal.pone.0206887.t004

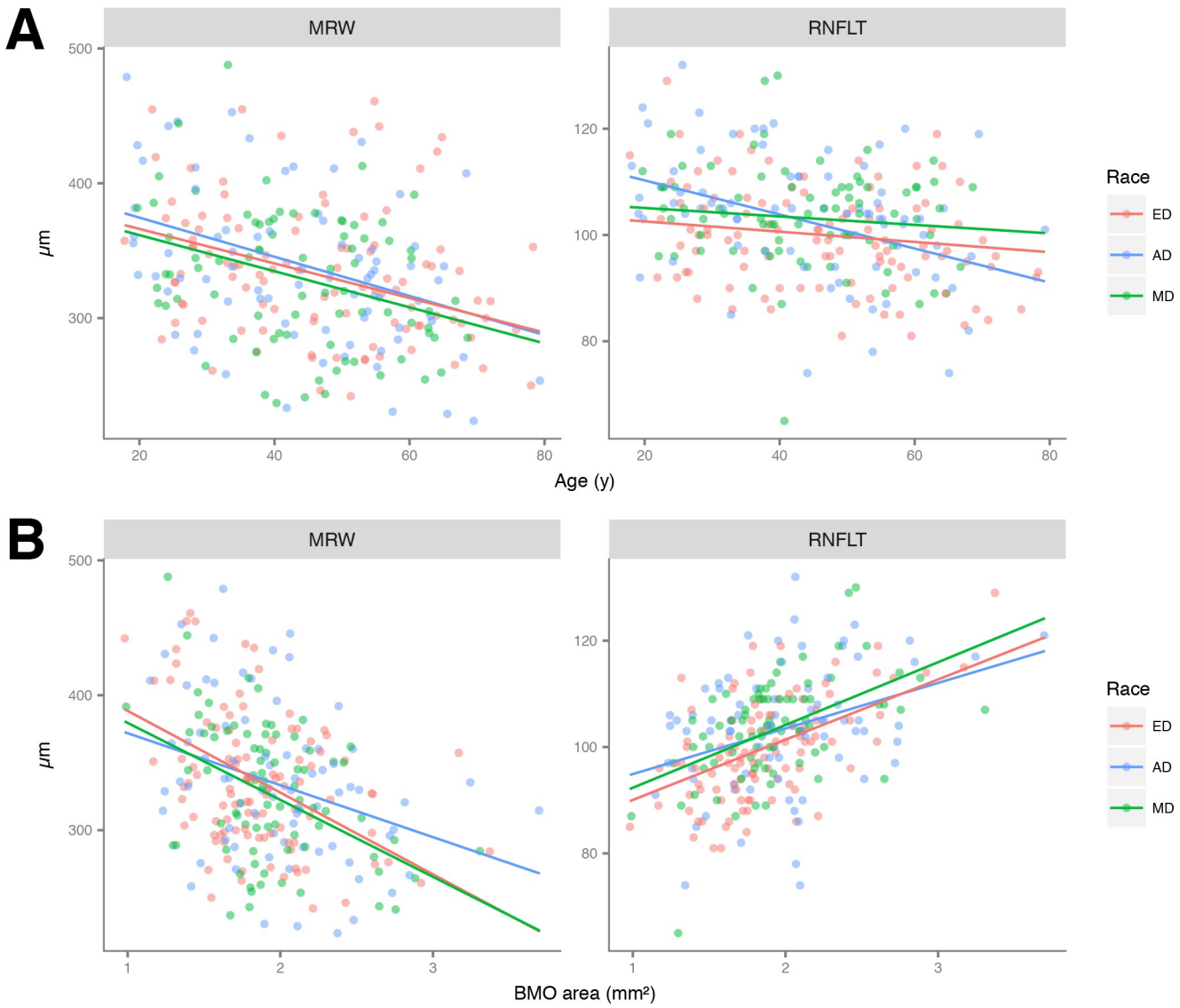

Fig 4. (A) Scatterplots showing the relationship between global minimum rim width (MRW) and age (left) and global peripapillary retinal nerve fiber layer thickness (RNFLT) and age (right), by racial group. Lines represent the coefficients of multivariable regression, adjusted for Bruch's membrane opening area. (B) Scatterplots showing the relationship between global minimum rim width (MRW) and Bruch's membrane opening (BMO) area (left) and global peripapillary retinal nerve fiber layer thickness (RNFLT) and BMO area (right) by racial group. Lines represent the coefficients of multivariable regression, adjusted for age. ED: European Descent; AD: African Descent; MD: Mixed Descent.

https://doi.org/10.1371/journal.pone.0206887.g004

between ED and MD (P = 0.83). On the other hand, after adjusting for age, global RNFLT increased significantly with BMO area in AD (8.57 μm/mm^2) and this was not different in ED (11.33 μm/mm^2, P = 0.15) and MD (11.81 μm/mm^2, P = 0.26). The rates of global RNFLT reduction were also similar between ED and MD (P = 0.83) (Fig 4). Global RNFLT increased with MRW, after adjusting for BMO area and age. The adjusted rate was significant in AD (2.05 μm/μm) and did not differ from ED (1.60 μm/μm, P = 0.45) and MD (1.72 μm/μm, P = 0.61). The rates were also similar between ED and MD (P = 0.85) (Fig 5).

Sectorial age-related loss of MRW and RNFLT, adjusted for BMO area, are shown in Fig 6. In general, the sectorial age-related percentage decays were faster for MRW than RNFLT, and faster in RNFLT sectors of AD than other races.

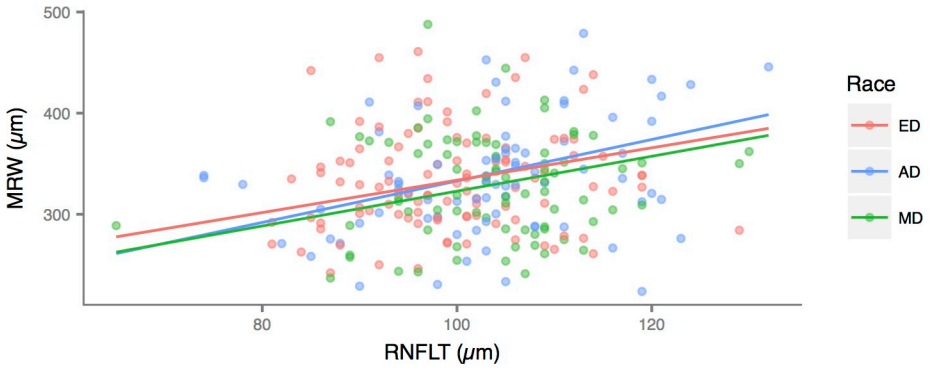

Fig 5. Scatterplot showing the relationship between global minimum rim width (MRW) and peripapillary retinal nerve fiber layer thickness (RNFLT) by racial group. The relationships did not differ among the three groups. ED: European Descent; AD: African Descent; MD: Mixed Descent.

https://doi.org/10.1371/journal.pone.0206887.g005

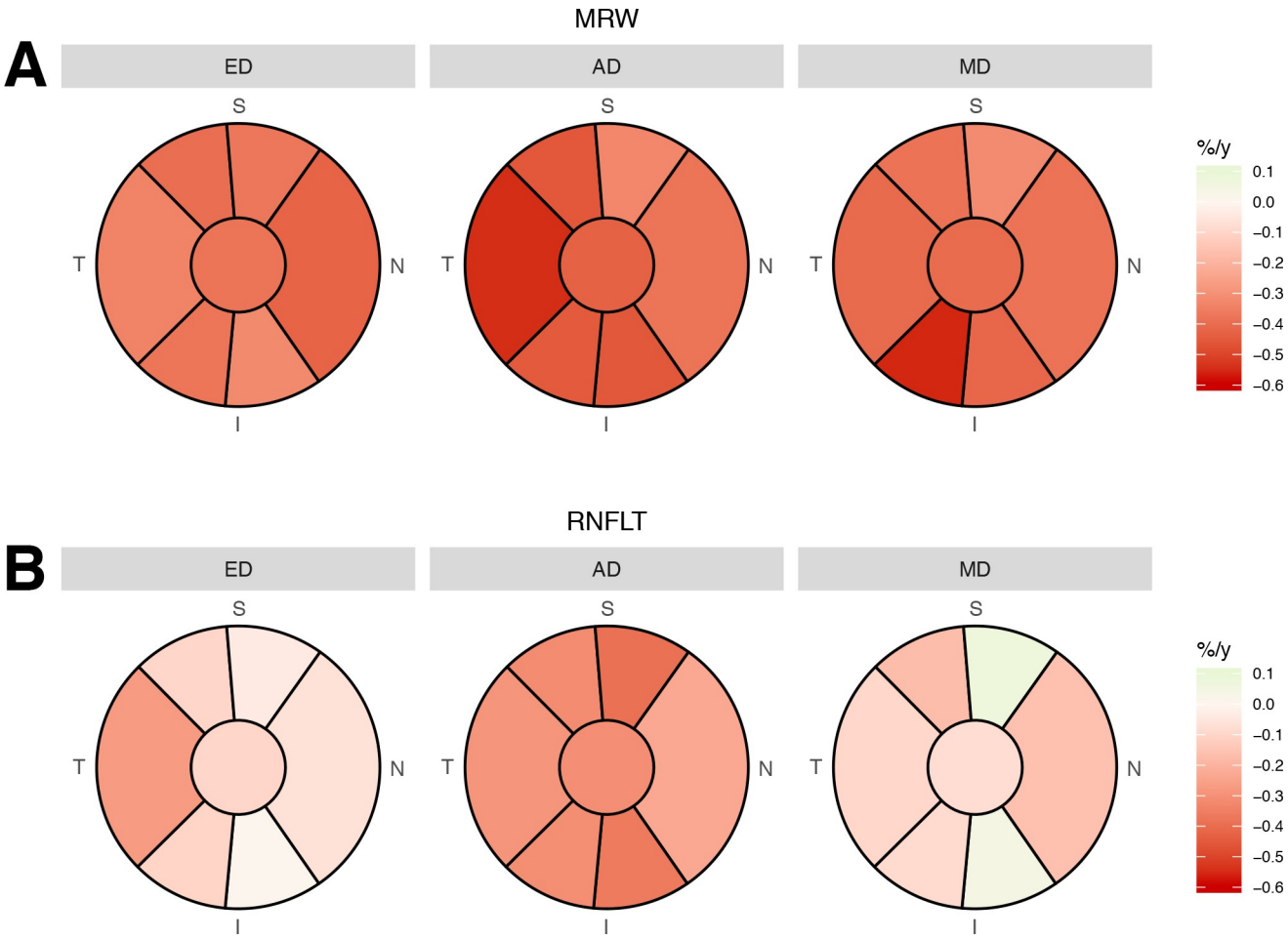

Fig 6. Graphs showing the sectorial age-related percentage decay (%/y) of (A) mean Bruch's membrane opening minimum rim width (MRW) and (B) peripapillary retinal nerve fiber layer thickness (RNFLT) globally (central circle) and in 6 sectors. Mean decay in each sector is color-coded according to the scale in the legend. ED: European Descent; AD: African Descent; MD: Mixed Descent.

https://doi.org/10.1371/journal.pone.0206887.g006

Table 5. Multivariable regression model evaluating the relationship between sectorial Minimum Rim Width (MRW) and peripapillary retinal nerve fiber layer thickness (RNFLT), adjusted for Bruch's membrane opening (BMO) area, age and race. Partial R squared estimating the relative importance of each predictor are given.

Sector	RNFL	Age	BMO Area	Race
Global	0.13	0.11	0.29	0.02
Temporal	0.03	0.07	0.08	0.01
Superotemporal	0.15	0.11	0.15	0.01
Inferotemporal	0.17	0.11	0.16	0.01
Nasal	0.08	0.11	0.30	0.01
Superonasal	0.11	0.08	0.22	0.01
Inferonasal	0.15	0.12	0.21	0.03

https://doi.org/10.1371/journal.pone.0206887.t005

The sectorial associations between MRW and RNFLT, adjusted for age, race and BMO area, were variable: it was highest in the inferotemporal sector ($R^2 = 0.17$) and lowest in the temporal sector ($R^2 = 0.03$). The relative importance of each covariate (RNFLT, age, race and BMO area) in MRW was variable between sectors. While BMO area was the most important predictor of MRW in all sectors, race was the covariable which least explained the variations in this parameter (**Table 5**).

Discussion

Numerous investigators have characterized racial differences in RNFLT and ONH parameters based on the clinically visible disc margin [17, 18]. Subsequently, there has been debate about the clinical relevance of these differences and the importance of race-specific databases in the evaluation of structural parameters for the diagnosis of glaucoma. Although previous studies did not report an enhanced performance when race-specific databases were used with OCT [27] and HRT [28–30], there is insufficient information about the influence of race on the newer ONH parameters based on BMO.

In this study, we evaluated ED, AD and MD individuals from Brazil and found no significant differences in global MRW and RNFLT among the three racial subgroups included in the study, with the exception that regionally, MRW was thicker in AD in the superonasal sector. Rhodes and colleagues recently compared MRW measurements between AD and ED in a US population and found no significant differences, both globally and regionally, between the two groups [16].

Regarding RNFLT, the three groups had similar global and regional values, except in the superonasal and inferonasal sectors, in which ED had statistically thinner RNFL measurements, even after adjusting for age and BMO area. Other authors have also shown similar global RNFLT between AD and ED, when adjusted for BMO area and when data was acquired and regionalized according to the FoBMO [16]. However, they have also reported significantly thinner temporal RNFLT in AD when compared to ED. In a study with RTVue, Girkin and colleagues also showed that AD from the US had significantly reduced RNFL thickness in the temporal sector and greater RNFL thickness in the superior and inferior regions compared with ED, after adjusting for age and disc area [18]. This previous study regionalized MRW and RNFLT measurements in four quadrants (superior, inferior, nasal and temporal) that were assigned relative to the horizontal axis of the acquired image frame. The location of these regions thus varies in each study eye. In the present study, we regionalized our data in six sectors that were consistently assigned in each study eye, relative to the axis connecting the fovea to BMO center. These differences in data regionalization may account for differences between our findings and previously published data.

In our study, the regional MRW and RNFLT distribution around BMO followed a similar pattern in AD, ED and MD individuals, confirming Rhodes et al findings for AD and ED from the US [16]. Also, similar to what has been previously described in other populations[14–16], the FoBMO angle also varied widely among Brazilian individuals, irrespective of race.

Previous studies in the US have consistently shown that AD have larger optic discs areas when compared to ED, when evaluated in postmortem measurements [31], disc photos [32], OCT [18, 33] and HRT [34–36]. In all these studies, optic disc area was measured based on the clinically visible optic disc margin. However, recently, it has also been shown that eyes of AD from the US have larger BMO areas than ED eyes, in contrast to the findings in our study. As mentioned before, Brazilian ADs come from different African territories compared to US ADs [20–22]. On the other hand, it is also possible that the genetic admixture of the Brazilian population contributed to a more homogeneous ONH phenotype across the racial groups [37, 38]. Finally, these discrepancies may be explained by inaccuracies of the self-reported nature of race definitions employed in all these studies.

Both MRW and RNFLT were correlated with BMO area, which was expected, since there is consistent evidence showing a decrease in MRW with an increase in BMO area [15, 16]. RNFLT in our study, on the other hand, increases significantly with an increase in BMO area. The underlying reasons for this are not entirely clear. One possible explanation is that RNFLT measurements are made closer to the BMO when a fixed (3.5 mm) circular scan is used in an eye with a large BMO area [39]. Another possible explanation is that individuals with large BMO areas may have a greater number of ganglion cells axons, as suggested in histologic studies [31, 40]. Finally, it is possible that eyes with larger BMO areas may have greater amounts of non-axonal components (i.e. glia).

In the present study, all racial groups showed similar rates of MRW decay with age, but AD had significantly higher rates of global RNFLT decay, compared to the other racial groups, a finding that has not been reported in the US population. Rhodes and colleagues described similar rates of MRW and RNFLT decay with age between ED and AD from the US [16], but the specific rates (in μm per year) were not reported. The higher rates of RNFLT decline with age in Brazilian AD eyes, and its underlying causes, may separately contribute to the higher prevalence [41–44] and earlier onset of glaucoma [45–47] in AD eyes. Although most of the population-based studies data have been reported in AD subjects from the US population, there is some evidence of higher prevalence of glaucoma among AD Brazilians[48]. The earlier onset of glaucoma in AD individuals is thought to be the result of a complex interaction of factors, including intraocular pressure, ONH and ocular biomechanics [46]. It is possible that the material properties of the ONH connective tissues of AD individuals differ from ED, leading to greater susceptibility to damage and, subsequently, to greater loss of ganglion cells with age. Regarding the age-related decay of global MRW and RNFLT in ED from the US, Canada and Europe, Chauhan and colleagues reported yearly rates of -1.34 and -0.21 μm/year, respectively [15]. The yearly rate of MRW decay was similar in our ED group, but the yearly decay of RNFLT was lower than what has been reported (-1.28 and -0.10 μm/year, respectively). However, it is important to note that the decay rates, in both studies, were highly variable among individuals (with large CIs), much more than the mean differences between our ED group and the ED group from the US.

Although statistically significant, the correlation between global MRW and global RNFLT was not strong, and was also variable by sector, after correction for BMO area and age. Although this finding is somewhat surprising, since it is expected for both the neuroretinal rim and the peripapillary RNFL to be constituted of the same retinal ganglion cells axons, it may be that differences in the non-axonal constituents of MRW and RNFLT, such as glial tissues and vessels, contribute to a lack of better correlation between these two parameters [49–

51]. It is also possible that the spatial correlation between the RNFL and the ONH rim is not perfect and, therefore, the number of axons in the peripapillary retina in a given sector may not be the same number of axons that constitute the ONH rim in that same sector. The correlation between these two parameters seems to be more complex than expected. Chauhan and colleagues reported similar findings[15]. Patel and colleagues also have already reported a non-linear relationship between them [52].

There are some limitations in our study. Only few individuals over the age of 70 were included in the study, especially in the MD and AD groups, which could impact the differences in age-related MRW and RNFLT decay rates across racial groups. In addition, the self-reported nature of the racial definition is also a source of error because self-reported race may not truly correspond to the real genetic composition of individuals [38, 53–56]. However, even the definition of race based on genetic findings is controversial [57], and the majority of population-based studies rely on self-reported racial definitions [18, 58].

While we described differences in some of the mean MRW and RNFLT sectorial measurements in AD, MD and ED from Brazil, these differences were small compared to the normal variations in ONH structure within each race. Therefore, there is a suggestion that a race-specific normative database may not be necessary. It may well be that non-race-specific databases with larger number of individuals will provide narrower 95% CIs than race-specific ones, actually increasing diagnostic accuracy when used compared to race-specific databases. In clinical practice, it means that when evaluating a glaucoma suspect, the comparison between patient's data to a race-specific normative database may not add to the diagnostic capability of the method. However, this may not be true for detection of progression. Age-related thinning of the RNFLT was significantly higher in the AD subgroup, which warrants further studies.

Supporting information

S1 File.
(CSV)

S2 File.
(CSV)

S3 File.
(CSV)

Author Contributions

Conceptualization: Camila S. Zangalli, Claude F. Burgoyne, Balwantray C. Chauhan, Vital P. Costa.

Data curation: Camila S. Zangalli, Jayme R. Vianna, Jamil Miguel-Neto.

Formal analysis: Camila S. Zangalli, Jayme R. Vianna, Alexandre S. C. Reis, Vital P. Costa.

Funding acquisition: Camila S. Zangalli, Vital P. Costa.

Investigation: Camila S. Zangalli, Jamil Miguel-Neto.

Methodology: Camila S. Zangalli, Claude F. Burgoyne, Balwantray C. Chauhan, Vital P. Costa.

Project administration: Camila S. Zangalli, Vital P. Costa.

Resources: Vital P. Costa.

Supervision: Camila S. Zangalli, Vital P. Costa.

Validation: Camila S. Zangalli.

Visualization: Alexandre S. C. Reis.

Writing – original draft: Camila S. Zangalli, Vital P. Costa.

Writing – review & editing: Jayme R. Vianna, Alexandre S. C. Reis, Claude F. Burgoyne, Balwantray C. Chauhan.

References

1. Armaly MF. Lessons to be learned from a glaucoma survey. J Iowa State Med Soc. 1960; 50:501–7. Epub 1960/08/01. PMID: 13794265.
2. Tan JC, Hitchings RA. Reference plane definition and reproducibility in optic nerve head images. Investigative ophthalmology & visual science. 2003; 44(3):1132–7. Epub 2003/02/26. PMID: 12601040.
3. Burk RO, Vihanninjoki K, Bartke T, Tuulonen A, Airaksinen PJ, Volcker HE, et al. Development of the standard reference plane for the Heidelberg retina tomograph. Graefe's archive for clinical and experimental ophthalmology = Albrecht von Graefes Archiv fur klinische und experimentelle Ophthalmologie. 2000; 238(5):375–84. Epub 2000/07/20. PMID: 10901468.
4. Hu Z, Abramoff MD, Kwon YH, Lee K, Garvin MK. Automated segmentation of neural canal opening and optic cup in 3D spectral optical coherence tomography volumes of the optic nerve head. Investigative ophthalmology & visual science. 2010; 51(11):5708–17. Epub 2010/06/18. https://doi.org/10.1167/iovs.09-4838 PMID: 20554616; PubMed Central PMCID: PMCPMC3061507.
5. Mwanza JC, Oakley JD, Budenz DL, Anderson DR, Cirrus Optical Coherence Tomography Normative Database Study G. Ability of cirrus HD-OCT optic nerve head parameters to discriminate normal from glaucomatous eyes. Ophthalmology. 2011; 118(2):241–8 e1. Epub 2010/10/06. https://doi.org/10.1016/j.ophtha.2010.06.036 PMID: 20920824; PubMed Central PMCID: PMCPMC3017237.
6. Poli A, Strouthidis NG, Ho TA, Garway-Heath DF. Analysis of HRT images: comparison of reference planes. Investigative ophthalmology & visual science. 2008; 49(9):3970–5. Epub 2008/05/13. https://doi.org/10.1167/iovs.08-1764 PMID: 18469180.
7. Reis AS, Sharpe GP, Yang H, Nicolela MT, Burgoyne CF, Chauhan BC. Optic disc margin anatomy in patients with glaucoma and normal controls with spectral domain optical coherence tomography. Ophthalmology. 2012; 119(4):738–47. https://doi.org/10.1016/j.ophtha.2011.09.054 PMID: 22222150; PubMed Central PMCID: PMC3319857.
8. Strouthidis NG, Yang H, Fortune B, Downs JC, Burgoyne CF. Detection of optic nerve head neural canal opening within histomorphometric and spectral domain optical coherence tomography data sets. Investigative ophthalmology & visual science. 2009; 50(1):214–23. https://doi.org/10.1167/iovs.08-2302 PMID: 18689697; PubMed Central PMCID: PMC2726821.
9. Povazay B, Hofer B, Hermann B, Unterhuber A, Morgan JE, Glittenberg C, et al. Minimum distance mapping using three-dimensional optical coherence tomography for glaucoma diagnosis. Journal of biomedical optics. 2007; 12(4):041204. https://doi.org/10.1117/1.2773736 PMID: 17867793.
10. Reis AS, O'Leary N, Yang H, Sharpe GP, Nicolela MT, Burgoyne CF, et al. Influence of clinically invisible, but optical coherence tomography detected, optic disc margin anatomy on neuroretinal rim evaluation. Investigative ophthalmology & visual science. 2012; 53(4):1852–60. https://doi.org/10.1167/iovs.11-9309 PMID: 22410561; PubMed Central PMCID: PMC3995560.
11. Chauhan BC, O'Leary N, Almobarak FA, Reis AS, Yang H, Sharpe GP, et al. Enhanced detection of open-angle glaucoma with an anatomically accurate optical coherence tomography-derived neuroretinal rim parameter. Ophthalmology. 2013; 120(3):535–43. https://doi.org/10.1016/j.ophtha.2012.09.055 PMID: 23265804; PubMed Central PMCID: PMC3667974.
12. Gardiner SK, Ren R, Yang H, Fortune B, Burgoyne CF, Demirel S. A method to estimate the amount of neuroretinal rim tissue in glaucoma: comparison with current methods for measuring rim area. American journal of ophthalmology. 2014; 157(3):540–9 e1-2. https://doi.org/10.1016/j.ajo.2013.11.007 PMID: 24239775; PubMed Central PMCID: PMCPMC3944716.
13. Chauhan BC, Burgoyne CF. From clinical examination of the optic disc to clinical assessment of the optic nerve head: a paradigm change. American journal of ophthalmology. 2013; 156(2):218–27 e2. https://doi.org/10.1016/j.ajo.2013.04.016 PMID: 23768651; PubMed Central PMCID: PMC3720683.
14. He L, Ren R, Yang H, Hardin C, Reyes L, Reynaud J, et al. Anatomic vs. acquired image frame discordance in spectral domain optical coherence tomography minimum rim measurements. PloS one. 2014;

9(3):e92225. https://doi.org/10.1371/journal.pone.0092225 PMID: 24643069; PubMed Central PMCID: PMC3958478.

15. Chauhan BC, Danthurebandara VM, Sharpe GP, Demirel S, Girkin CA, Mardin CY, et al. Bruch's Membrane Opening Minimum Rim Width and Retinal Nerve Fiber Layer Thickness in a Normal White Population: A Multicenter Study. Ophthalmology. 2015; 122(9):1786–94. https://doi.org/10.1016/j.ophtha.2015.06.001 PMID: 26198806; PubMed Central PMCID: PMCPMC4698808.
16. Rhodes LA, Huisingh CE, Quinn AE, McGwin G Jr., LaRussa F, Box D, et al. Comparison of Bruch's Membrane Opening Minimum Rim Width Among Those With Normal Ocular Health by Race. American journal of ophthalmology. 2017; 174:113–8. https://doi.org/10.1016/j.ajo.2016.10.022 PMID: 27825982; PubMed Central PMCID: PMCPMC5253316.
17. Marsh BC, Cantor LB, WuDunn D, Hoop J, Lipyanik J, Patella VM, et al. Optic nerve head (ONH) topographic analysis by stratus OCT in normal subjects: correlation to disc size, age, and ethnicity. J Glaucoma. 2010; 19(5):310–8. https://doi.org/10.1097/IJG.0b013e3181b6e5cd PMID: 19855299; PubMed Central PMCID: PMCPMC3417149.
18. Girkin CA, McGwin G Jr., Sinai MJ, Sekhar GC, Fingeret M, Wollstein G, et al. Variation in optic nerve and macular structure with age and race with spectral-domain optical coherence tomography. Ophthalmology. 2011; 118(12):2403–8. https://doi.org/10.1016/j.ophtha.2011.06.013 PMID: 21907415.
19. IBGE. Características étnico-raciais da população: classificações e identidades 2013 [06/15/2017]. Available from: http://biblioteca.ibge.gov.br/index.php/biblioteca-catalogo?view=detalhes&id=263405.
20. Goncalves VF, Carvalho CM, Bortolini MC, Bydlowski SP, Pena SD. The phylogeography of African Brazilians. Hum Hered. 2008; 65(1):23–32. https://doi.org/10.1159/000106059 PMID: 17652961.
21. Mathias RA, Taub MA, Gignoux CR, Fu W, Musharoff S, O'Connor TD, et al. A continuum of admixture in the Western Hemisphere revealed by the African Diaspora genome. Nat Commun. 2016; 7:12522. https://doi.org/10.1038/ncomms12522 PMID: 27725671; PubMed Central PMCID: PMCPMC5062574 other authors declare no competing financial interests.
22. Montinaro F, Busby GB, Pascali VL, Myers S, Hellenthal G, Capelli C. Unravelling the hidden ancestry of American admixed populations. Nat Commun. 2015; 6:6596. https://doi.org/10.1038/ncomms7596 PMID: 25803618; PubMed Central PMCID: PMCPMC4374169.
23. Reis ASC, Zangalli CES, Abe RY, Silva AL, Vianna JR, Vasconcellos JPC, et al. Intra- and interobserver reproducibility of Bruch's membrane opening minimum rim width measurements with spectral domain optical coherence tomography. Acta Ophthalmol. 2017; 95(7):e548–e55. Epub 2017/06/27. https://doi.org/10.1111/aos.13464 PMID: 28650590.
24. Garway-Heath DF, Poinoosawmy D, Fitzke FW, Hitchings RA. Mapping the visual field to the optic disc in normal tension glaucoma eyes. Ophthalmology. 2000; 107(10):1809–15. PMID: 11013178.
25. Kutner MH. Applied linear statistical models. 5th ed. Boston: McGraw-Hill Irwin; 2005. xxviii, 1396 p. p.
26. R Development Core Team. R—A Language and Environment for Statistical Computing: R—Foundation for Statistical Computing. 2011.
27. Girkin CA, Liebmann J, Fingeret M, Greenfield DS, Medeiros F. The effects of race, optic disc area, age, and disease severity on the diagnostic performance of spectral-domain optical coherence tomography. Investigative ophthalmology & visual science. 2011; 52(9):6148–53. https://doi.org/10.1167/iovs.10-6698 PMID: 21421879.
28. Rao HL, Babu GJ, Sekhar GC. Comparison of the diagnostic capability of the Heidelberg Retina Tomographs 2 and 3 for glaucoma in the Indian population. Ophthalmology. 2010; 117(2):275–81. https://doi.org/10.1016/j.ophtha.2009.06.062 PMID: 19969365.
29. Tan XL, Yap SC, Li X, Yip LW. Comparison of Ethnic-specific Databases in Heidelberg Retina Tomography-3 to Discriminate Between Early Glaucoma and Normal Chinese Eyes. Open Ophthalmol J. 2017; 11:40–6. https://doi.org/10.2174/1874364101711010040 PMID: 28400890; PubMed Central PMCID: PMCPMC5362979.
30. Zelefsky JR, Harizman N, Mora R, Ilitchev E, Tello C, Ritch R, et al. Assessment of a race-specific normative HRT-III database to differentiate glaucomatous from normal eyes. J Glaucoma. 2006; 15(6):548–51. https://doi.org/10.1097/01.ijg.0000212289.00917.a8 PMID: 17106370.
31. Quigley HA, Brown AE, Morrison JD, Drance SM. The size and shape of the optic disc in normal human eyes. Archives of ophthalmology. 1990; 108(1):51–7. PMID: 2297333.
32. Varma R, Tielsch JM, Quigley HA, Hilton SC, Katz J, Spaeth GL, et al. Race-, age-, gender-, and refractive error-related differences in the normal optic disc. Archives of ophthalmology. 1994; 112(8):1068–76. PMID: 8053821.
33. Girkin CA, Sample PA, Liebmann JM, Jain S, Bowd C, Becerra LM, et al. African Descent and Glaucoma Evaluation Study (ADAGES): II. Ancestry differences in optic disc, retinal nerve fiber layer, and

macular structure in healthy subjects. Archives of ophthalmology. 2010; 128(5):541–50. https://doi.org/10.1001/archophthalmol.2010.49 PMID: 20457974; PubMed Central PMCID: PMCPMC2910255.

34. Girkin CA, McGwin G Jr., Long C, DeLeon-Ortega J, Graf CM, Everett AW. Subjective and objective optic nerve assessment in African Americans and whites. Investigative ophthalmology & visual science. 2004; 45(7):2272–8. PMID: 15223805.

35. Girkin CA, McGwin G Jr., McNeal SF, DeLeon-Ortega J. Racial differences in the association between optic disc topography and early glaucoma. Investigative ophthalmology & visual science. 2003; 44 (8):3382–7. PMID: 12882785.

36. Racette L, Boden C, Kleinhandler SL, Girkin CA, Liebmann JM, Zangwill LM, et al. Differences in visual function and optic nerve structure between healthy eyes of blacks and whites. Archives of ophthalmology. 2005; 123(11):1547–53. https://doi.org/10.1001/archopht.123.11.1547 PMID: 16286617.

37. Saloum de Neves Manta F, Pereira R, Vianna R, Rodolfo Beuttenmuller de Araujo A, Leite Goes Gitai D, Aparecida da Silva D, et al. Revisiting the genetic ancestry of Brazilians using autosomal AIM-Indels. PloS one. 2013; 8(9):e75145. https://doi.org/10.1371/journal.pone.0075145 PMID: 24073242; PubMed Central PMCID: PMCPMC3779230.

38. Suarez-Kurtz G, Pena SD, Struchiner CJ, Hutz MH. Pharmacogenomic Diversity among Brazilians: Influence of Ancestry, Self-Reported Color, and Geographical Origin. Front Pharmacol. 2012; 3:191. https://doi.org/10.3389/fphar.2012.00191 PMID: 23133420; PubMed Central PMCID: PMCPMC3490152.

39. Savini G, Zanini M, Carelli V, Sadun AA, Ross-Cisneros FN, Barboni P. Correlation between retinal nerve fibre layer thickness and optic nerve head size: an optical coherence tomography study. Br J Ophthalmol. 2005; 89(4):489–92. https://doi.org/10.1136/bjo.2004.052498 PMID: 15774930; PubMed Central PMCID: PMCPMC1772588.

40. Jonas JB, Schmidt AM, Muller-Bergh JA, Schlotzer-Schrehardt UM, Naumann GO. Human optic nerve fiber count and optic disc size. Investigative ophthalmology & visual science. 1992; 33(6):2012–8. PMID: 1582806.

41. Coleman AL, Miglior S. Risk factors for glaucoma onset and progression. Surv Ophthalmol. 2008; 53 Suppl1:S3–10. Epub 2008/12/17. https://doi.org/10.1016/j.survophthal.2008.08.006 PMID: 19038621.

42. Friedman DS, Jampel HD, Munoz B, West SK. The prevalence of open-angle glaucoma among blacks and whites 73 years and older: the Salisbury Eye Evaluation Glaucoma Study. Archives of ophthalmology. 2006; 124(11):1625–30. https://doi.org/10.1001/archopht.124.11.1625 PMID: 17102012.

43. Tielsch JM, Katz J, Singh K, Quigley HA, Gottsch JD, Javitt J, et al. A population-based evaluation of glaucoma screening: the Baltimore Eye Survey. Am J Epidemiol. 1991; 134(10):1102–10. PMID: 1746520.

44. Tielsch JM, Sommer A, Katz J, Royall RM, Quigley HA, Javitt J. Racial variations in the prevalence of primary open-angle glaucoma. The Baltimore Eye Survey. JAMA. 1991; 266(3):369–74. PMID: 2056646.

45. Sommer A, Tielsch JM, Katz J, Quigley HA, Gottsch JD, Javitt JC, et al. Racial differences in the cause-specific prevalence of blindness in east Baltimore. N Engl J Med. 1991; 325(20):1412–7. https://doi.org/10.1056/NEJM199111143252004 PMID: 1922252.

46. Khachatryan N, Medeiros FA, Sharpsten L, Bowd C, Sample PA, Liebmann JM, et al. The African Descent and Glaucoma Evaluation Study (ADAGES): predictors of visual field damage in glaucoma suspects. American journal of ophthalmology. 2015; 159(4):777–87. https://doi.org/10.1016/j.ajo.2015.01.011 PMID: 25597839; PubMed Central PMCID: PMCPMC4361282.

47. Leske MC, Connell AM, Wu SY, Nemesure B, Li X, Schachat A, et al. Incidence of open-angle glaucoma: the Barbados Eye Studies. The Barbados Eye Studies Group. Archives of ophthalmology. 2001; 119(1):89–95. PMID: 11146731.

48. Sakata K, Sakata LM, Sakata VM, Santini C, Hopker LM, Bernardes R, et al. Prevalence of glaucoma in a South brazilian population: Projeto Glaucoma. Investigative ophthalmology & visual science. 2007; 48 (11):4974–9. https://doi.org/10.1167/iovs.07-0342 PMID: 17962447.

49. Ogden TE. Nerve fiber layer astrocytes of the primate retina: morphology, distribution, and density. Investigative ophthalmology & visual science. 1978; 17(6):499–510. PMID: 96038.

50. Ogden TE. Nerve fiber layer of the primate retina: thickness and glial content. Vision research. 1983; 23 (6):581–7. PMID: 6612997.

51. Onda E, Cioffi GA, Bacon DR, Van Buskirk EM. Microvasculature of the human optic nerve. American journal of ophthalmology. 1995; 120(1):92–102. PMID: 7611333.

52. Patel NB, Sullivan-Mee M, Harwerth RS. The relationship between retinal nerve fiber layer thickness and optic nerve head neuroretinal rim tissue in glaucoma. Investigative ophthalmology & visual science.

2014; 55(10):6802–16. https://doi.org/10.1167/iovs.14-14191 PMID: 25249610; PubMed Central PMCID: PMCPMC4214209.

53. Leite TK, Fonseca RM, de Franca NM, Parra EJ, Pereira RW. Genomic ancestry, self-reported "color" and quantitative measures of skin pigmentation in Brazilian admixed siblings. PloS one. 2011; 6(11): e27162. https://doi.org/10.1371/journal.pone.0027162 PMID: 22073278; PubMed Central PMCID: PMCPMC3206941.

54. Parra FC, Amado RC, Lambertucci JR, Rocha J, Antunes CM, Pena SD. Color and genomic ancestry in Brazilians. Proc Natl Acad Sci U S A. 2003; 100(1):177–82. https://doi.org/10.1073/pnas.0126614100 PMID: 12509516; PubMed Central PMCID: PMCPMC140919.

55. Pimenta JR, Zuccherato LW, Debes AA, Maselli L, Soares RP, Moura-Neto RS, et al. Color and genomic ancestry in Brazilians: a study with forensic microsatellites. Hum Hered. 2006; 62(4):190–5. https://doi.org/10.1159/000096872 PMID: 17106202.

56. Suarez-Kurtz G, Vargens DD, Struchiner CJ, Bastos-Rodrigues L, Pena SD. Self-reported skin color, genomic ancestry and the distribution of GST polymorphisms. Pharmacogenet Genomics. 2007; 17 (9):765–71. https://doi.org/10.1097/FPC.0b013e3281c10e52 PMID: 17700365.

57. Jorde LB, Wooding SP. Genetic variation, classification and 'race'. Nat Genet. 2004; 36(11 Suppl): S28–33. https://doi.org/10.1038/ng1435 PMID: 15508000.

58. Knight OJ, Girkin CA, Budenz DL, Durbin MK, Feuer WJ, Cirrus OCTNDSG. Effect of race, age, and axial length on optic nerve head parameters and retinal nerve fiber layer thickness measured by Cirrus HD-OCT. Archives of ophthalmology. 2012; 130(3):312–8. https://doi.org/10.1001/archopthalmol.2011.1576 PMID: 22411660.